Adaptive transmitter for seasonal variations of the underwater acoustic channel in the Black Sea

GEORGE ZARNESCU
Department of Electronics and Telecommunications
Maritime University of Constanța
Mircea cel Batran St, no. 104, Constanța, 900663
ROMANIA
zarnescugeorge@yahoo.com

Abstract: - It is known that a slight change in the speed of sound underwater will modify the properties of the underwater acoustic channel (UAC). The diurnal and nocturnal changes of the sound speed profile (SSP) will determine the UAC to be highly variable. This variability has a negative impact on the performance of an underwater acoustic modem (UAM). Therefore we must take into account the daily changes of the sound speed profile when we design an UAM. Developed in this way an underwater communication device will transmit efficiently and reliably to the surface the acquired scientific data.
In this article we present diurnal and nocturnal mean sound speed profiles for each season computed using conductivity, temperature and depth (CTD) data acquired in the north-western region of the Black Sea from 1889 to 1998. The CTD information was obtained from the NOAA's oceanographic and atmospheric database. Then AcTUP simulation software was used to create the model of the underwater acoustic medium and to obtain the daily frequency response changes of the UAC for each season, for the region of interest. Based on these results we propose an adaptive architecture for an analog transmitter which could be used in the analog front-end of an UAM.

Key-Words: - Sound Speed Profile, Underwater Acoustic Channel, Channel Modeling, Channel Simulation, Frequency Dependent Simulation and Adaptive Transmitter Architecture**.**

1 Introduction

An underwater acoustic modem is a communication device used to transmit the acquired scientific data through the underwater medium to the surface. Such a device is equipped with batteries which could store a finite amount of energy. This energy must be used efficiently to ensure a long time operation of UAM. In [1] was shown that an efficient way to use this energy is to adapt the UAM to the underwater acoustic channel.

The existing commercial [2] and research modems [3] have a fixed architecture and transmit the acquired data at a single central frequency. If they are used in long term monitoring operations the highly variable UAC will make them unreliable most of the time. A slight change of the sound speed profile will modify the frequency response of the UAC therefore the mean daily changes of the SSP could be taken into account when an UAM is designed.

It is known the fact that an UAM operates remotely and the underwater environment is harsh with the devices deployed by humans for scientific research.

If a researcher wants to modify the parameters of an UAM to compensate the daily changes of the SSP he must bring the modem to the surface, make the appropriate hardware changes and bring it back into the sea. This is a difficult and costly task. If the UAM operates in an underwater wireless sensor network (UWSN) the hardware changes must be done for each modem and the operation costs will be higher.

Combining the classical analog components with digital potentiometers one could design an analog transmitter with an adaptive architecture which could be used in the analog front-end of an underwater acoustic modem. It is expected afterwards an increase in the reliability of the UAM to daily changes of the UAC. Additionally this device will use efficiently the finite amount of energy in the batteries because it will be adapted to the particular underwater acoustic channel.

In this article we present a daily mean of the sound speed profile for each season based on data acquired in the north-western region of the Black Sea from 1889 to 1998. In this region we find the continental shelf of the Black Sea. In Figure 1 we

show the location of his area and the distribution of sound speed profiles.

The SSPs were obtained from the NOAA's oceanographic and atmospheric database [4]. Information about the geophysical properties of the seafloor was obtained from [5], [6].

The daily mean SSPs and the properties of the seafloor sediments were used to create a simulation model of the underwater acoustic channel for the area of interest. The model was composed in Matlab with the use of Acoustic Toolbox User interface and Post processor (AcTUP) plug-in. This program was used also to simulate the propagation of underwater sound waves [7].

In section 2 we characterize our region of interest. We highlight the statistics of the region, the diurnal and nocturnal mean SSP for each season and the composition of the seafloor sedimentary layers. In section 3 we present our underwater acoustic channel model. Also here we will emphasize the daily changes in the frequency response of the UAC. In section 4 we present the architecture of the analog transmitter designed based on the results from section 3. In section 5 we present the conclusions of this article and the future work.

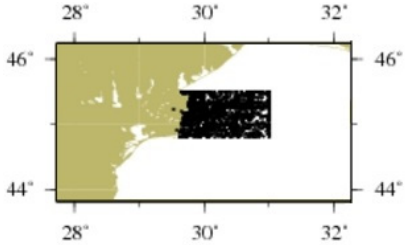

Fig. 1 – North-western region of the Black Sea and the distribution of the sound speed profiles.

2 Daily mean of the SSP and seafloor properties

The region of interest is shown in Figure 1. It is geographically located between 44.8 E and 45.0 E longitudes and between 29.5 N and 31.0 N latitudes. This surface has a length of 137 km, a width of 68 km and an area of 9316 km. In this region were recorded 4560 sound speed profiles therefore we have one measurement on an area of 2 km^2. The average depth is 27 m with a standard deviation of 13 m.

2.1 Daily mean of the SSP

In Figure 2 the daily mean of the sound speed profile is shown for each season. The diurnal SSPs are represented with blue and the nocturnal SSPs are shown in red. The sound speed profiles were computed using the equation 1 and the CTD data obtained from NOAA's oceanographic and atmospheric database.

$$c(T,S,z) = 1449.2 + 4.6 \cdot T - 0.055 \cdot T^2 + 0.00029 \cdot T^3 + (1.34 - 0.01 \cdot T) \cdot (S - 35) + 0.016 \cdot z \quad (1)$$

where c is the speed of sound in m/s, T is the temperature in degrees Celsius, S is salinity in parts per thousand (ppt or $^{o}/_{oo}$) and z is the depth measured in meters [8]. This equation is valid for $0^{o} \leq T \leq 35^{o}$ C, $0 \leq S \leq 45\ ^{o}/_{oo}$ and $0 \leq z \leq 1000$ m

We observe in Figure 2 that the sound speed is less than 1500 m/s, the average sound speed in water. This is due to the fact that the average salinity in the area of interest, 17 ppt, is much smaller than the average salinity, 35 ppt. The low salinity is due to the fresh water brought by the Danube into the Black Sea.

During winter between 0 and 30 m we observe the mixed layer (the temperature is constant with depth) which is due to the harsh weather conditions. Below 30 m we have a negative temperature gradient which is called the thermocline (a decrease in temperature or velocity with depth). The nocturnal sound speed is smaller than the diurnal sound speed because of the lower temperatures during the night.

In Figure 2 b) during the night we observe only the thermocline. This is due to a decrease in temperature with depth. During the day between 0 and 30 m the thermocline is still present. Below 30 m we notice a positive gradient which means we have a region with constant temperature.

During summer because of the calm and sunny conditions which lasts during a whole day we notice the thermocline. We see that the diurnal and nocturnal SSPs can be interchangeable.

In the fall between 0 and 10 m we notice the occurrence of the mixed layer which is due to worsening the meteorological conditions. Below 10 m we observe the thermocline.

2.2 Seafloor SSP and geophysical properties

The seafloor consists of three sediment layers. The first layer is composed of silty-clay or mud. We must specify that this is a dynamic sedimentary layer which consists of river deposits continuously brought by the Danube. The second layer consists of silt and the third layer is made of sand.

In Figure 3 we show the sound speed profile of the seafloor sedimentary layers. We specify that the third sedimentary layer is deeper than 1 m. The

geophysical properties for each layer are presented in Table 1.

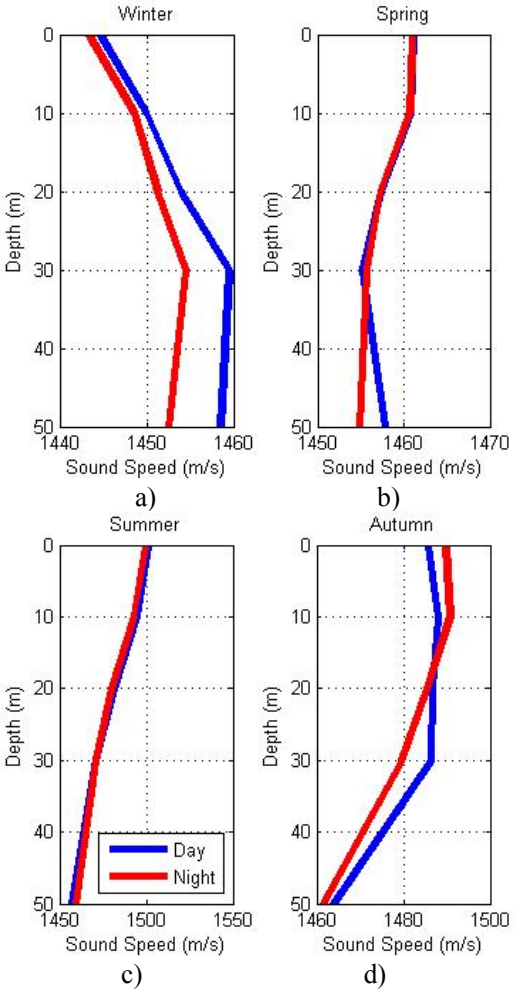

Fig. 2 – Daily mean of the sound speed profile for each season.

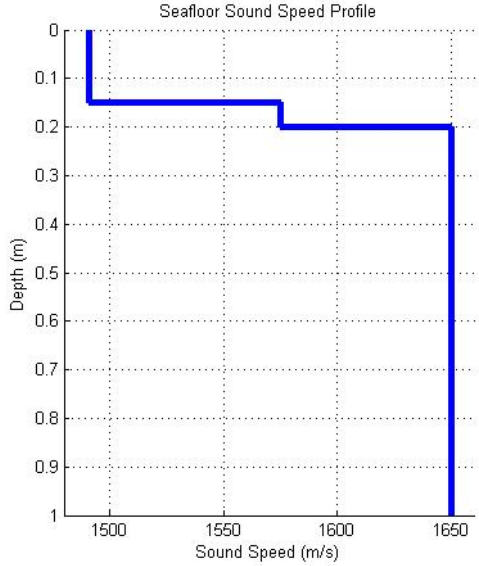

Fig. 3 – Seafloor sound speed profile.

Table 1 – Geophysical properties of the seafloor sediments.

Properties	Silty-Clay	Silt	Sand
Depth (m)	0.15	0.05	> 1
Sound speed (m/s)	1491	1575	1650
Density (kg/m^3)	1480	1700	1900
Seafloor attenuation (dB/λ)	0.15	1	0.8

3 UAC modeling and simulation

We simulated using AcTUP an underwater wireless sensor network consisting of two underwater acoustic modems placed on the seafloor in a horizontal link.

In the next subsections we show our UAC physical model and the simulation results of the sound propagation underwater.

3.1 Channel modeling

In Figure 4 we present our underwater acoustic channel model created with AcTUP software. The sea surface was considered a reflector with a rms roughness of 1.75 m. The bottom was modeled as a flat reflector and attenuator. The sea depth is considered to be 40 m (the mean sea depth plus one standard deviation). The transmitter and the receiver were placed at 50 cm above the seafloor in a horizontal configuration. The transmission distance between them is 500 m.

Using the information in Figure 2, Figure 3 and Table 1 eight channel simulation models were created. For each simulation model we defined the same bottom configuration.

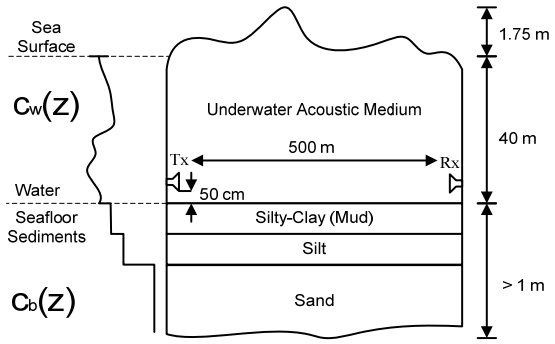

Fig. 4 – Black Sea underwater acoustic channel model. z is the sea depth measured in meters, $c_w(z)$ represents the water SSP and $c_b(z)$ the seafloor SSP.

3.2 Channel simulation

Using the UAC model presented in subsection 3.1 we performed a frequency dependent simulation in AcTUP. This software allows the use of several algorithms which could be used to characterize the propagation of sound waves in an acoustic medium. The simulation results were obtained using the Bounce-Bellhop algorithm.

AcTUP runs first the Bounce program. This algorithm uses the information from Table 1 and creates a file with brc extension. In this file we find the values of the **b**ottom **r**eflection **c**oefficient depending on the grazing angle. Then AcTUP runs Bellhop program, which is a ray tracing algorithm. The Bellhop inputs are brc file and the simulation parameters defined in subsection 3.1. Bellhop writes the ray tracing results in a file with arr extension. In this file we find the amplitude delay profile for each ray path and for each transmission distance.

AcTUP runs Bounce-Bellhop algorithm for each transmission frequency. We emphasize that the algorithm offers good results for high frequencies. In equation 2 we present an empirical formula which was used to find the minimum simulation frequency [9].

$$f > 20 \cdot \frac{v}{z} \qquad (2)$$

We know that the depth (z) is 40 m and the maximum sound speed (v) is 1462 m/s hence the minimum simulation frequency is 731 Hz. In our simulations we used a minimum frequency of 1 kHz.

We simulated our underwater acoustic channel in the frequency range 1-99 kHz with a step of 1 kHz and we obtained 99 arr files. Those files represent 99 UAC impulse responses, one for each simulation frequency. Using the equation 3 we computed the underwater acoustic channel frequency response for our transmission distance and for the eight channel simulation models.

$$H(l,f) = \sum_{k=1}^{n} A_{k,l} \cdot e^{j\theta_{k,l}} \cdot e^{-j2\pi f t_{k,l}} \qquad (3)$$

In equation 3 $A_{k,l}$ is the amplitude and $\theta_{k,l}$ is the phase of the impulse response. $t_{k,l}$ represents the delay of each impulse or the time of arrival relative to the first impulse. All three parameters are dependent on the channel geometry, simulation frequency and transmission distance. Therefore the transfer function is also dependent on the transmission distance and transmission frequency.

In Figure 5 we show the dependence of the amplitude of the weight function on the transmission frequency. The impulse responses were obtained for the winter nocturnal sound speed profile. The impulse response in Figure 5 a) was obtained at a frequency of 1 kHz and the impulse response in Figure 5 b) was obtained at a frequency of 99 kHz. We observe that an increase in the transmission frequency will produce an increase in the impulse amplitudes.

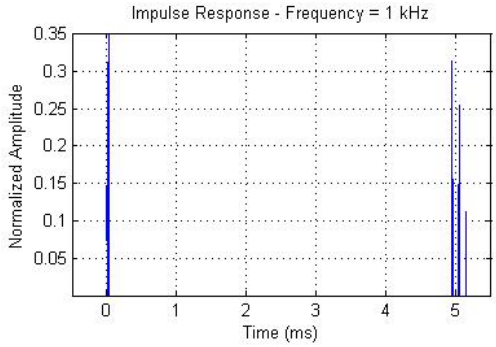

a)

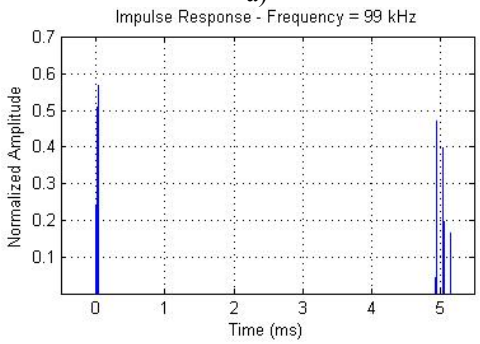

b)

Fig. 5 – The dependence of the amplitude of the weight function on the transmission frequency.

3.3 UAC diurnal and nocturnal total frequency response

In this subsection we define two important underwater acoustic channel parameters, namely transmission loss and noise level.

The parameter transmission loss, TL, was computed using equation 4 and the results from section 3.2.

$$TL = 10\log_{10}|H(f)|^2 \qquad (4)$$

The noise level, NL, was computed using equation 5 for a transmission frequency between 1kHz and 99 kHz and for a wind speed (w) of 10 m/s.

$$NL = 50 + 7.5w^{0.5} + 20\log_{10} f - 40\log_{10}(f + 0.4) \qquad (5)$$

A wind speed of 10 m/s means there are waves with moderate heights. The Beaufort number for this wind speed is 5 and the wind description is fresh breeze. The rms wave height is 1.75 m.

The total frequency response, TFR, was computed using equation 6

$$TFR = TL + NL \quad (6)$$

which is the sum of transmission loss and noise level. The sum operation is legal because our parameters have units of decibels relative to the intensity of a plane wave of rms pressure of 1μPa.

In Figure 6 we show the diurnal and nocturnal total frequency responses for each season.

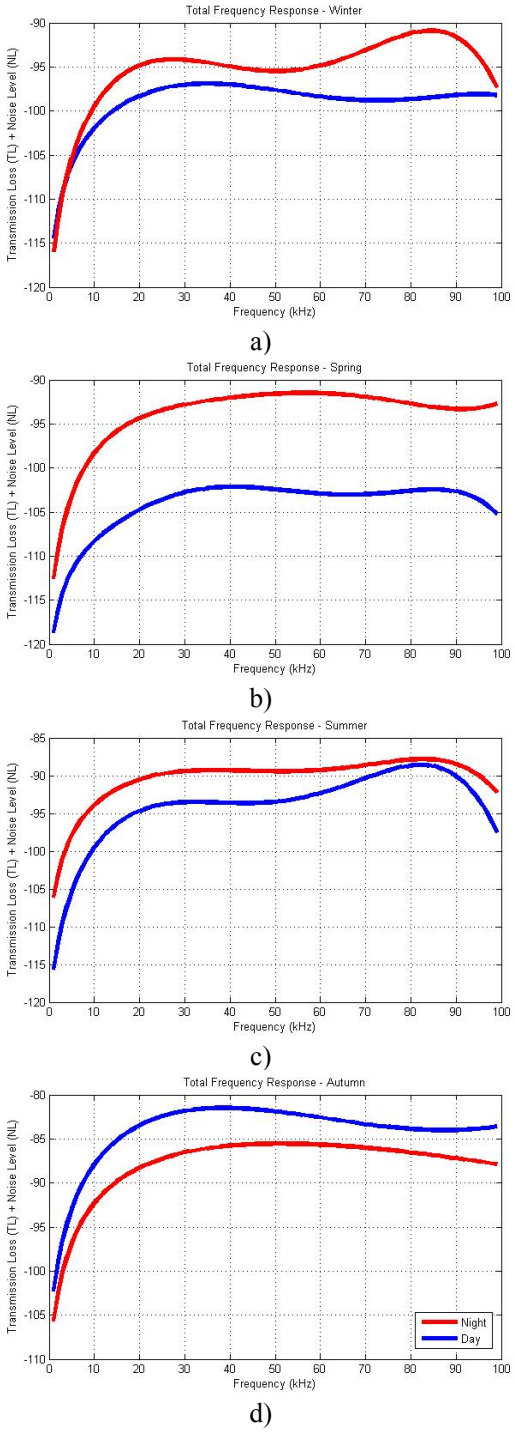

Fig. 6 – Diurnal and nocturnal total frequency responses for each season.

In the above figure we observe that each TFR acts as a bandpass filter. We can find a central frequency were the amplitude is highest. Around that frequency we can find a minimum and a maximum frequency for which the maximum amplitude decreases by 3 dB [10].

We note that the TFR has an irregular behavior. The central frequency and the 3 dB bandwidth are highly variable. We can observe this behavior in Figure 6 a). The nocturnal central frequency is around 85 kHz and the diurnal central frequency is around 35 kHz. Therefore we have a frequency shift of 50 kHz. The nocturnal bandwidth is greater than the diurnal bandwidth. In Table 2 we summarize the results shown in Figure 6.

Table 2 – Summary of the results shown in Figure 6.

	f_c(kHz) (correct ones)	Δf_{3dB} (kHz)	TFR (dB)	TVR (dB)	K (V/V)
Winter day	35 (43)	8.4	-97 (-43-41)	149 (146)	5 (3.6)
Winter night	84 (49)	2.8	-91 (-39-40)	142 (141)	5.6 (3.6)
Spring day	41 (44)	7.9	-102 (-51-41)	147 (143)	11.2 (12.7)
Spring night	57 (35)	7.9	-92 (-41-43)	146 (150)	4 (2.3)
Summer day	82 (53)	2.8	-89 (-39-39)	144 (143)	3.5 (2.6)
Summer night	83 (89)	7.7	-88 (-40-35)	144 (140)	3.2 (2.6)
Autumn day	39 (41)	8.2	-82 (-38-41)	148 (148)	1 (1.6)
Autumn night	51 (59)	7.9	-86 (-37-38)	144 (141)	2.5 (2.3)

4 Adaptive transmitter architecture

Based on the results shown in Table 2 we design a transmitter with an adaptive architecture for an underwater acoustic modem.

We used the passive sonar equation, which is shown in equation 7, to compute the transmitter amplifications. These are shown in Table 2. SNR is the signal-to-noise ratio, TVR is the transmission voltage response of the projector, ΔB the

transmission bandwidth and K is the amplification. The rms input voltage, V_{rms}, is equal to 1 V.

$$SNR = TVR + 20 \cdot \log_{10}(K \cdot V_{rms}) - TL - NL - 10 \cdot \log_{10}(\Delta B) \quad (7)$$

Than we designed using Matlab's signal processing toolbox, eight 4th order Chebyshev filters for the central frequencies shown in Table 2 and with a bandwidth of 10 kHz. We must specify that each filter was transformed in a two stage configuration, each stage representing a 2nd order filter.

We implemented these filters using the Sallen-Key bandpass filter topology. The transmitter architecture is shown in Figure 7. We created four adaptive filters for each season. Than we can change the values of the digital potentiometers R_1, R_f, R_a and R_b to match the diurnal and nocturnal total frequency response for a season.

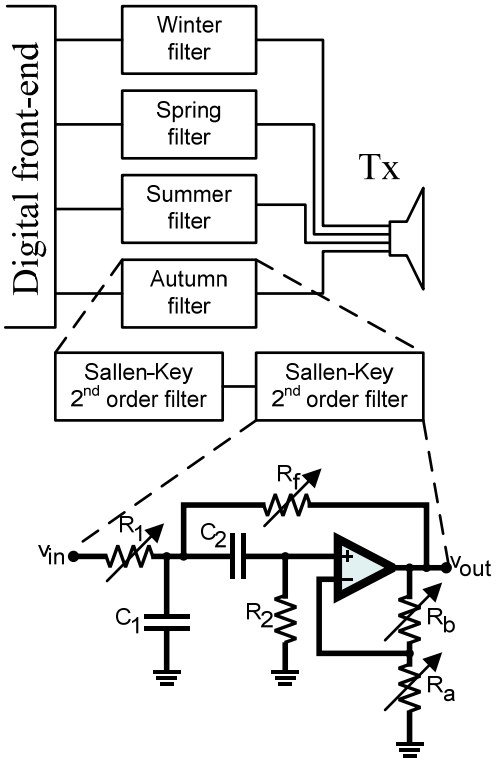

Fig. 7 – Adaptive transmitter architecture.

The values of the passive components were computed with the equations (8)-(12). First we fixed the values of C_1, C_2 and R_2, then we changed the value of g to provide the right amplification. Afterwards we obtained the values of R_1 and R_f. At the end we chose appropriate values for R_a and R_b.

$$a = (2\pi f_c)^2 R_2 C_1 C_2 \quad (8)$$

$$b = C_1\left(2\pi\Delta B - \frac{1}{R_2(C_1 + C_2)}\right) \quad (9)$$

$$g = \frac{R_a}{R_b} \quad (10)$$

$$R_1 = \frac{1+g}{b + a \cdot g} \quad (11)$$

$$R_f = \frac{1+g}{a-b} \quad (12)$$

5 Conclusions

In this article we show the modifications of the frequency response of the underwater acoustic channel to changes in the daily mean of the sound speed profile for each season. We present diurnal and nocturnal mean sound speed profiles in the region of interest, which is located in the north-western part of the Black Sea. Using AcTUP simulation software we modeled a particular underwater channel and obtained the underwater sound propagation results. Using these results we computed the changes of frequency response of the underwater acoustic channel for each season.

Based on these results we designed an analog transmitter with an adaptive architecture for an underwater acoustic modem.

In the near future we want to install in the considered region an underwater wireless sensor network consisting of two modems placed on the bottom in a horizontal link. These modems will operate for a year to test the efficiency of the analog transmitter.

References:

[1] Zărnescu, G., Low Cost adaptive underwater acoustic modem for the Black Sea environment, *ATOM-N*, 2012.

[2] Benthos, Inc. Underwater acoustic modems, http://www.benthos.com, 2012.

[3] Benson, B., Design of a Low-Cost Underwater Acoustic Modem, *IEEE Embedded Systems Letters*, Vol.2, No.3, 2010, pp. 58-61.

[4] National Oceanic and Atmospheric Administration, http://www.noaa.gov/, 2012.

[5] Oaie, Ghe. and Secrieru, D., Black Sea Basin: Sediment Types and Distribution, Sedimentation processes, *Proceedings of Euro-EcoGeoCentre-Romania*, 2004.

[6] Jensen, F. B., *Computational Ocean Acoustics*, 2nd edition, Springer, 2011.

[7] Maggi, A. M., AcTUP v 2.2, Acoustic Toolbox User-interface and Post-processor, Installation and User Guide, 2010.

[8] Brekhovskikh, L. M., *Fundamentals of Ocean Acoustics*, 3rd edition, Springer, 2003.

[9] Porter, M. B., The Bellhop Manual and User's Guide, 2011.
[10] Stojanovic, M., On the Relationship between Capacity and Distance in an Underwater Acoustic Communication Channel, *ACM SIGMOBILE Mobile Computing and Communications Review*, Vol. 11, No. 4, 2007, pp.33-43.